crystals

MDPI

Article

Ternary Copper(II) Coordination Compounds with Nonpolar Amino Acids and 2,2′-Bipyridine: Monomers vs. Polymers

Darko Vušak [1], Katarina Ležaić [1,2], Nenad Judaš [1] and Biserka Prugovečki [1,*]

[1] Division of General and Inorganic Chemistry, Department of Chemistry, Faculty of Science, University of Zagreb, Horvatovac 102a, 10000 Zagreb, Croatia; dvusak@chem.pmf.hr (D.V.); k.lezaic@uu.nl (K.L.); judas@chem.pmf.hr (N.J.)

[2] Organic Chemistry and Catalysis, Institute for Sustainable and Circular Chemistry, Faculty of Science, Utrecht University, 3584 CG Utrecht, The Netherlands

* Correspondence: biserka@chem.pmf.hr

Abstract: Reactions of copper(II) sulfate with 2,2′-bipyridine (bipy) and amino acids with nonpolar side chains (L-alanine (HAla), L-valine (HVal), or L-phenylalanine (HPhe)) were investigated under different solution-based and mechanochemical methods. Five new ternary coordination compounds were obtained by a solution-based synthesis and three of them additionally by the liquid-assisted mechanochemical method: $\{[Cu(\mu\text{-L-Ala})(H_2O)(bipy)]_2SO_4\cdot 2H_2O\}_n$ (**1a·2H$_2$O**), $\{[Cu(\mu\text{-L-Ala})(H_2O)(bipy)][Cu(\text{L-Ala})(H_2O)(bipy)]SO_4\cdot 2.5H_2O\}_n$ (**1b·2.5H$_2$O**), $\{[Cu(\mu\text{-L-Val})(H_2O)(bipy)][Cu(\text{L-Val})(H_2O)(bipy)]_3(SO_4)_2\cdot 4H_2O\}_n$ (**2·4H$_2$O**), [Cu(L-Phe)(H$_2$O)(bipy)][Cu(L-Phe)(SO$_4$)(bipy)]·8H$_2$O (**3·8H$_2$O**), and [Cu(L-Phe)(H$_2$O)(bipy)][Cu(L-Phe)(SO$_4$)(bipy)]·9H$_2$O (**3·9H$_2$O**). The compounds were characterized by single-crystal and powder X-ray diffraction, infrared spectroscopy, and a thermal analysis. Structural studies revealed two structural types, monomeric in **3·8H$_2$O** and **3·9H$_2$O**, polymeric architectures in **1a·2H$_2$O**, and mixed structures (monomeric and polymeric) in **1b·2.5H$_2$O** and **2·4H$_2$O**. The copper(II) ion is either pentacoordinated or hexacoordinated, with an observed Jahn–Teller effect. The crystal structures are based on an intensive network of hydrogen bonds and π interactions. **1a·2H$_2$O** and **2·4H$_2$O** showed substantial in vitro antiproliferative activity toward human hepatocellular carcinoma (HepG2) and moderate activity toward human acute monocytic leukemia cell lines (THP-1).

Keywords: 2,2′-bipyridine; amino acids; coordination polymers; copper; crystal structures; mechanochemistry; solution-based synthesis; ternary coordination compounds

check for updates

Citation: Vušak, D.; Ležaić, K.; Judaš, N.; Prugovečki, B. Ternary Copper(II) Coordination Compounds with Nonpolar Amino Acids and 2,2′-Bipyridine: Monomers vs. Polymers. *Crystals* **2024**, *14*, 656. https://doi.org/10.3390/cryst14070656

Academic Editor: Ana M. Garcia-Deibe

Received: 21 June 2024
Revised: 12 July 2024
Accepted: 15 July 2024
Published: 17 July 2024

Copyright: © 2024 by the authors. Licensee MDPI, Basel, Switzerland. This article is an open access article distributed under the terms and conditions of the Creative Commons Attribution (CC BY) license (https://creativecommons.org/licenses/by/4.0/).

1. Introduction

Copper is an essential element in living organisms that appears in traces and participates in many biochemical processes (respiration, metabolism, DNA synthesis, and oxidation-reduction reactions) [1]. Copper(II) compounds that contain biological ligands like amino acids are currently studied because of their wide spectrum of applications in biomedicine [1–4], crystal engineering [5–7], catalysis in organic chemistry [8], and stereospecific reactions [8–10].

After the discovery of cisplatin [11], great attention has been given to the transition metal coordination compounds with a similar biological activity, especially to the ternary copper(II) compounds with amino acids and *N*,*N*′-donor heterocyclic bases such as 2,2′-bipyridine or 1,10-phenanthroline derivatives. It was shown that the presence of heterocyclic bases, which act as *N*–*N* ligands, stabilizes the molecular structure and is crucial for antiproliferative activity [1]. These compounds belong to the group of compounds called *Casiopeinas*, which stand out because of their antiproliferative properties and can be used as cytotoxic or diagnostic agents as well as antitumor or antiviral medicine [1,12,13]. The antiproliferative properties arise from DNA binding abilities in the physiological

conditions with covalent or non-covalent interactions (groove binding, intercalation, and external electrostatic effects) [14,15]. In addition to drug developments, these types of compounds can be used as model compounds for studying the interaction between DNA and proteins [15]. In most copper(II) coordination compounds, amino acids coordinate to copper atoms as *N*,*O* didentate ligands, utilizing the amino group and the carboxylate, but due to different side chains, amino acids are additionally capable of taking part in the non-covalent interactions, mostly in the formation of hydrogen bonds and π interactions [6,16]. In such a way, many different architectures with different dimensionalities (0-dimensional monomers, 1D polymer chains, and 2D or 3D networks) may emerge from the self-assembly. Additionally, these compounds are very often in the form of different solvates, containing porous structures, making them interesting compounds for molecular recognition and the absorption of gases or solvents [6,17].

Several monomeric and polymeric crystal structures of copper(II) with 2,2′-bipyridine with nonpolar amino acids (L-alanine, L-valine, and L-phenylalanine) containing different anions (nitrate, perchlorate, or hexafluorophosphate) have been structurally characterized so far [17–26]. In all the reported crystal structures, the geometry around the copper(II) atom is either a distorted square pyramidal or octahedral. Most of this research, including those and similar ternary coordination compounds, was conducted to reveal their structure and biological activity [27–30]. It was also found that the copper(II) coordination compound with 2,2′-bipyridine and L-alanine has long-lived photoluminescence and a high quantum yield under air exposure [20]. The copper(II) coordination compound with 2,2′-bipyridine and L-valine was evaluated as a functional model for the catechol oxidase enzyme and phenoxazinone synthase [23]. It was found that the ternary coordination compound of copper(II) with 2,2′-bipyridine and L-phenylalanine has excellent ferroelectric and piezoelectric properties [25,26].

Recently, we reported syntheses, structures, and magnetic and biological properties of a series of ternary copper(II) coordination compounds with amino acids (L-serine, L-threonine, and glycine) and heterocyclic *N*,*N*′-donor ligands (2,2′-bipyridine and 1,10-phenanthroline) [6,31,32].

In this work, we were interested in reactions of copper(II) sulfate with 2,2′-bipyridine (bipy) and nonpolar amino acids (L-alanine (HAla), L-valine (HVal), and L-phenylalanine (HPhe)) under different solution-based and mechanochemical synthetic methods. The effects of different solvents (water and methanol) and different amino acid side chains on crystallization and crystal structures were investigated. These studies revealed different structural types, including monomeric and polymeric architectures, as well as different solvatomorphs. Five new ternary copper(II) compounds with 2,2′-bipyridine (bipy) and nonpolar amino acids (L-alanine (HAla), L-valine (HVal), or L-phenylalanine (HPhen)— {[Cu(μ-L-Ala)(H_2O)(bipy)]$_2SO_4$·2H_2O}$_n$ (**1a·2H_2O**), {[Cu(μ-L-Ala)(H_2O)(bipy)][Cu(L-Ala)(H_2O)(bipy)]SO_4·2.5H_2O}$_n$ (**1b·2.5H_2O**), {[Cu(μ-L-Val)(H_2O)(bipy)][Cu(L-Val)(H_2O)(bipy)]$_3$(SO_4)$_2$·4H_2O}$_n$ (**2·4H_2O**), [Cu(L-Phe)(H_2O)(bipy)][Cu(L-Phe)(SO_4)(bipy)]·8H_2O (**3·8H_2O**) and [Cu(L-Phe)(H_2O)(bipy)][Cu(L-Phe)(SO_4)(bipy)]·9H_2O (**3·9H_2O**)) were synthesized and structurally and thermally characterized.

2. Materials and Methods

The copper(II) sulfate pentahydrate was purchased from Gram-mol; 2,2′-bipyridine from Acros Organics; L-alanine, L-valine, and L-phenylalanine from Fisher Bioreagents; and methanol from Carlo Erba Reagents. The copper(II) hydroxide was prepared by a method described in the literature [33,34]. A Retch MM200 ball mill was used for grinding experiments, working at a frequency of 25 Hz, with Teflon jars (volume of 14 mL) and stainless-steel grinding balls (diameter of 8 mm). For a thermogravimetric analysis, the Mettler Toledo TGA/DSC 3+ was used under an oxygen flow of 50 mL min^{-1} and a heating rate of 10 °C min^{-1} in the temperature range of 25–800 °C. The sample (approximately 8.3–15.5 mg) was placed in a standard alumina crucible (70 μL). IR(ATR) spectra were

measured using a Thermo Scientific™ Nicolet™ iS50 FTIR Spectrometer in ATR mode in the range of 4000–400 cm^{-1}.

General procedure for solution-based syntheses. Copper(II) hydroxide (0.25 mmol); copper(II) sulfate pentahydrate (0.25 mmol); 2,2′-bipyridine (0.5 mmol); amino acids (L-alanine, L-valine, or L-phenylalanine—0.5 mmol); and a solvent (water, methanol, or a mixture of water and methanol—10 mL) were mixed. The solution was heated until most of the reactants were dissolved. The reaction mixture was filtered off if some precipitate was left after approximately one hour.

General procedure for liquid-assisted grinding (LAG) mechanochemical syntheses. Copper(II) sulfate pentahydrate (0.25 mmol); 2,2′-bipyridine (0.5 mmol); copper(II) hydroxide (0.25 mmol); and amino acids (L-alanine, L-valine, or L-phenylalanine—0.5 mmol) were placed in a Teflon milling jar (volume 14 mL) with one stainless steel ball (diameter of 8 mm). Liquids (water or methanol) were used with η = 0.2 μL mg^{-1}. The milling time was 15 min.

Solution-based synthesis of $\{[Cu(\mu\text{-L-Ala})(H_2O)(bipy)]_2SO_4 \cdot 2H_2O\}_n$ **(1a·2H$_2$O).** A mixture of 2,2′-bipyridine (80.6 mg and 0.5 mmol), L-alanine (45.2 mg and 0.5 mmol), copper(II) sulfate pentahydrate (62.1 mg and 0.25 mmol), copper(II) hydroxide (23.8 mg and 0.25 mmol), and methanol (10 mL) was heated until a clear dark blue solution appeared. The obtained solution slowly evaporated at room temperature, and after a few days, dark blue needle-like crystals of **1a·2H$_2$O** formed, which were of good quality for single-crystal X-ray diffraction. Synthesis is not always reproducible, since **1b·2.5H$_2$O** might also crystallize in these synthetic conditions. The crystal data for **1a·2H$_2$O**, $C_{26}H_{36}Cu_2N_6O_{12}S$ (M = 783.77 g mol^{-1}) are as follows: monoclinic; space group $C2$ (no. 5); a = 22.2598(4) Å; b = 7.0109(1) Å; c = 22.6682(5) Å; β = 116.481(2)°; V = 3166.47(11) $Å^3$; Z = 4; T = 170(2) K; μ(MoKα) = 1.481 mm^{-1}; D_{calc} = 1.644 g cm^{-3}; 47,713 reflections measured (5.2° ≤ 2Θ ≤ 60.0°); and 9236 unique ones (R_{int} = 0.021 and R_{sigma} = 0.013), which were used in all calculations. The final R_1 was 0.0220 ($I > 2\sigma(I)$), and wR_2 was 0.0633 (all data).

Solution-based synthesis of $\{[Cu(\mu\text{-L-Ala})(H_2O)(bipy)][Cu(\text{L-Ala})(H_2O)(bipy)]SO_4 \cdot 2.5H_2O\}_n$ **(1b·2.5H$_2$O).** Copper(II) hydroxide (25.3 mg and 0.25 mmol), copper(II) sulfate pentahydrate (62.3 mg and 0.25 mmol), 2,2′-bipyridine (78.6 mg and 0.5 mmol), and L-alanine (44.6 mg and 0.5 mmol) were dissolved in water (10 mL) and heated until a clear solution was obtained. The dark blue solution was left to cool down and evaporate slowly at room temperature. After a few days or weeks, dark blue prismatic crystals of **1b·2.5H$_2$O** were formed. Crystals were suitable for single-crystal X-ray diffraction. The crystal data for **1b·2.5H$_2$O**, $C_{52}H_{74}Cu_4N_{12}O_{25}S_2$ (M = 1585.51g mol^{-1}) are as follows: orthorhombic; space group $P2_12_12$ (no. 18); a = 7.2476(3) Å; b = 18.9871(5) Å; c = 23.4551(6) Å; V = 3227.68(18) $Å^3$; Z = 2; T = 295(2) K; μ(MoKα) = 1.455 mm^{-1}; D_{calc} = 1.631 g cm^{-3}; 16,263 reflections measured (8.6° ≤ 2Θ ≤ 52.0°); and 6303 unique ones (R_{int} = 0.024 and R_{sigma} = 0.040), which were used in all calculations. The final R_1 was 0.0493 ($I > 2\sigma(I)$), and wR_2 was 0.1408 (all data).

IR (ATR) for **1b·2.5H$_2$O**: $\tilde{\nu}$/cm^{-1}: 3426 (m), 3205 (w), 3115 (m), 3093 (m), 3079 (m), 3063 (m), 3041 (m), 2983 (m), 2970 (m), 2931 (m), 1691 (w), 1619 (m), 1609 (ms), 1601 (s), 1576 (m), 1569 (m), 1496 (w), 1477 (m), 1458 (m), 1442 (ms), 1396 (ms), 1367 (m), 1319 (mw), 1295(w), 1252 (m), 1203(mw), 1150(m), 1125 (m), 1072 (vs), 1042 (s), 1033 (s), 1021 (s), 981 (m), 956 (m), 933 (mw), 911 (w), 899 (w), 860 (m), 807 (mw), 791 (w), 764 (s), 743 (m), 731 (s), 667 (m), 652 (m), 640 (m), 606 (s), 564 (ms), 557 (ms), 511 (ms), 500 (ms), 472 (m), 466 (m), 458 (m), 447 (m), 419 (s), and 411 (ms).

Solution-based synthesis of $\{[Cu(\mu\text{-L-Val})(H_2O)(bipy)][Cu(\text{L-Val})(H_2O)(bipy)]_3(SO_4)_2 \cdot 4H_2O\}_n$ (**2·4H$_2$O**). L-valine (59.3 mg and 0.5 mmol), 2,2′-bipyridine (78.4 mg and 0.5 mmol), copper(II) hydroxide (24.1 mg and 0.25 mmol), and copper(II) sulfate pentahydrate (63.1 mg and 0.25 mmol) were dissolved in water or methanol (10 mL) and heated for 45 min. The precipitate was filtered, and the dark blue filtrate was left to evaporate at room temperature for a few weeks until dark blue prismatic crystals of **2·4H$_2$O** were crystallized. Crystals were analyzed by single-crystal X-ray diffraction. The crystal data for **2·4H$_2$O**,

$C_{30}H_{44}Cu_2N_6O_{12}S$ (M = 839.85 g mol^{-1}) are as follows: monoclinic; space group $C2$ (no. 5); a = 41.7116(5) Å, b = 7.3630(1) Å; c = 22.3565(2) Å; β = 93.404(1)°; V = 6854.07(14) Å^3; Z = 8; T = 170(2) K; μ(MoKα) = 1.374 mm^{-1}; D_{calc} = 1.628 g cm^{-3}; 113,260 reflections measured (5.2° ≤ 2Θ ≤ 65.0°); and 24,013 unique ones (R_{int} = 0.025 and R_{sigma} = 0.018), which were used in all calculations. The final R_1 was 0.0473 ($I > 2\sigma(I)$), and wR_2 was 0.1286 (all data).

IR (ATR) for **2·4H$_2$O**: $\tilde{\nu}$/cm^{-1}: 3471 (m), 3205 (m), 3112 (m), 3078 (m), 2931 (m), 2896(m), 2875 (m), 1630 (s), 1610 (s), 1568 (m), 1498 (w), 1479 (m), 1444 (m), 1430 (m), 1392 (m), 1362 (m), 1321 (m), 1256(w), 1218(w), 1193(w), 1162(m), 1142 (w), 1089 (s), 1055 (s), 1042 (s), 1032 (s), 1020 (s), 989 (m) 973 (m), 957 (m), 940 (m), 934 (m), 901 (m), 856 (w), 850 (w), 810 (m), 767 (ms), 711 (ms), 722 (s), 663 (w), 652 (w), 637 (w), 616 (s), 548 (ms), 499 (w), 422 (s), and 408 (m).

Solution-based synthesis of [Cu(L-Phe)(H$_2$O)(bipy)][Cu(L-Phe)(SO$_4$)(bipy)]·8H$_2$O **(3·8H$_2$O).** L-phenylalanine (82.5 mg and 0.5 mmol), 2,2′-bipyridine (78.1 mg and 0.5 mmol), copper(II) hydroxide (24.4 mg and 0.25 mmol), and copper(II) sulfate pentahydrate (62.4 mg and 0.25 mmol) were dissolved in a mixture of water and methanol (10 mL, 1:9 v/v) and heated for 15 min. The precipitate was filtered, and the dark blue filtrate was left to evaporate at room temperature for a few days until dark blue prismatic crystals of **3·8H$_2$O** formed. The crystals were analyzed by single-crystal X-ray diffraction. If water is used as the solvent, a glass-like solid is formed upon evaporation of the solvent. The crystallization of **3·8H$_2$O** is highly dependent on external conditions, so in some experiments, [Cu(μ-L-Phe)$_2$]$_n$ was formed instead [35]. The crystal data for **3·8H$_2$O**, $C_{38}H_{54}Cu_2N_6O_{17}S$ (M = 1026.01 g mol^{-1}) are as follows: monoclinic; space group $P2_1$ (no. 4); a = 13.1976(2) Å; b = 31.6655(7) Å; c = 22.1043(4) Å; β = 103.992(2)°; V = 8963.5(3) Å^3; Z = 8; T = 170(2) K; μ(CuKα) = 2.282 mm^{-1}; D_{calc} = 1.521 g cm^{-3}; 166,988 reflections measured (5.0° ≤ 2Θ ≤ 150.0°); and 36,423 unique ones (R_{int} = 0.030 and R_{sigma} = 0.023), which were used in all calculations. The final R_1 was 0.0731 ($I > 2\sigma(I)$), and wR_2 was 0.2262 (all data).

IR (ATR) for **3·8H$_2$O**: $\tilde{\nu}$/cm^{-1}: 3333 (m), 3246 (m), 3152 (m), 3115 (m), 3086 (m), 3034 (m), 2934 (m), 2860(w), 2875 (m), 1619 (s), 1616 (s), 1609 (s), 1601 (s), 1575 (m), 1569 (m), 1496 (mw), 1475 (mw), 1445 (m), 1395 (m), 1347 (w), 1319 (m), 1270 (w), 1253(w), 1214(w), 1186(w), 1158(m), 1095 (ms), 1082 (s), 1056 (s), 1033 (s), 1021 (ms), 972 (m), 934 (w), 925 (w), 894 (w), 826 (w), 814 (w), 773 (s), 756 (m), 731 (s), 705 (s), 661 (m), 651 (w), 600 (s), 616 (s), 548 (ms), 499 (w), 476 (m), 465 (m), 415 (s), and 402 (m).

Solution-based synthesis of [Cu(L-Phe)(H$_2$O)(bipy)][Cu(L-Phe)(SO$_4$)(bipy)]·9H$_2$O **(3·9H$_2$O).** L-phenylalanine (82.4 mg and 0.5 mmol), 2,2′-bipyridine (77.9 mg and 0.5 mmol), copper(II) hydroxide (24.1 mg and 0.25 mmol), and copper(II) sulfate pentahydrate (62.4 mg and 0.25 mmol) dissolved in 10 mL of methanol, and the mixture was heated for 15 min. The precipitate was filtered, and the dark blue filtrate was left to evaporate at room temperature for a few days until dark blue prismatic crystals of **3·9H$_2$O** formed. Crystals were analyzed by single-crystal X-ray diffraction. The crystallization of **3·9H$_2$O** is highly dependent on external conditions, so in some cases, [Cu(μ-L-Phe)$_2$]$_n$ was formed instead [35]. The crystal data for **3·9H$_2$O**, $C_{38}H_{56}Cu_2N_6O_{18}S$ (M = 1044.01 g mol^{-1}) are as follows: monoclinic; space group $P2_1$ (no. 4); a = 11.0442(1) Å; b = 32.2410(4) Å; c = 13.0288(2) Å; β = 100.863(2)°; V = 4556.11(10) Å^3; Z = 4; T = 100(2) K; μ(MoKα) = 1.059 mm^{-1}; D_{calc} = 1.522 g cm^{-3}; 113,707 reflections measured (4.4° ≤ 2Θ ≤ 54.0°); and 19,857 unique ones (R_{int} = 0.036 and R_{sigma} = 0.020), which were used in all calculations. The final R_1 was 0.0685 ($I > 2\sigma(I)$), and wR_2 was 0.2058 (all data).

Liquid-assisted grinding (LAG) mechanochemical syntheses of 1b·2.5H$_2$O. 2,2′-bipyridine (78.2 mg and 0.5 mmol), copper(II) hydroxide (24.4 mg and 0.25 mmol), copper(II) sulfate pentahydrate (62.3 mg and 0.25 mmol), L-alanine (44.3 mg and 0.5 mmol), and methanol (41.8 μL and η = 0.2 μL mg^{-1}) were placed in a Teflon jar with one stainless steel ball. Milling was carried out for 15 min at room temperature. The product was analyzed by powder X-ray diffraction, and the powder pattern was consistent with the pattern calculated from the single-crystal structure data of **1b·2.5H$_2$O** (Figure S1).

Liquid-assisted grinding (LAG) mechanochemical syntheses of 2·4H$_2$O. 2,2′-bipyridine (77.9 mg and 0.5 mmol), copper(II) hydroxide (24.5 mg and 0.25 mmol), copper(II) sulfate pentahydrate (62.6 mg and 0.25 mmol), L-valine (58.6 mg and 0.5 mmol), and water or methanol (44.7 μL and η = 0.2 μL mg^{-1}) were placed in a Teflon jar with one stainless steel ball. Milling was carried out for 15 min at room temperature. The product was analyzed by powder X-ray diffraction, and the powder pattern was consistent with the pattern calculated from the single-crystal structure data of **2·4H$_2$O** (Figure S2).

Liquid-assisted grinding (LAG) mechanochemical syntheses of 3·8H$_2$O. 2,2′-bipyridine (78.1 mg and 0.5 mmol), copper(II) hydroxide (24.4 mg and 0.25 mmol), copper(II) sulfate pentahydrate (62.4 mg and 0.25 mmol), L-phenylalanine (82.6 mg and 0.5 mmol), and water (49.5 μL and η = 0.2 μL mg^{-1}) were placed in a Teflon jar with one stainless steel ball. Milling was carried out for 15 min at room temperature. The product was analyzed by powder X-ray diffraction, and the TGA was conducted. The powder pattern was mostly consistent with the pattern calculated from the single-crystal structure data of **3·8H$_2$O** (Figure S3). Some additional peaks appeared, probably due to the slow decomposition of the sample over time, as seen in the changes in the diffraction pattern over time (Figure S3). The TGA of the same sample gave a water fraction close to the theoretical value for **3·8H$_2$O** (exp., 15.6%; theor., 15.8%).

Single-crystal X-ray Diffraction. The Oxford Diffraction Xcalibur 2 CCD diffractometer was used for a single-crystal X-ray diffraction analysis of **1b·2.5H$_2$O**, with a graphite monochromator and MoKα source of radiation (λ = 0.71073 Å) by a ω scan at room temperature. The XtaLAB Synergy-S diffractometer, at a temperature of 170 K and with MoK_α radiation (λ = 0.71073 Å), was used for the analysis of **1a·2H$_2$O**, **2·4H$_2$O**, and **3·9H$_2$O**, while CuK_α radiation (λ = 1.54184 Å) was used for the analysis of **3·8H$_2$O**. The collection and reduction of data were performed by the CrysAlis software package [36]. Crystal structures were solved using direct methods by SHELXS [37] and refined by the SHELXL [38] program, incorporated within the WinGX program system [39]. The structures were refined by the full-matrix least-squares method based on F^2 against all reflections. All non-hydrogen atoms were refined anisotropically. The hydrogen atoms of aminoacidates and 2,2′-bipyridine ligands were found in the Fourier difference map, but due to the poor geometry of some of them, they were placed on calculated positions for the corresponding functional group. Hydrogen atoms belonging to the water molecules were located in the Fourier difference map and were restrained to O–H and H···H distances of 0.85(1) Å and 1.39(2) Å, respectively. Some of the positional parameters of water hydrogen atoms were fixed to their position due to a disorder in the structure or instability of a model. Sulfate ions in **1a·2H$_2$O** are disordered and were modelled over two positions, with occupancies of exactly 0.5, since they lie on a two-fold axis. One sulfate ion and one valinate residue in **2·4H$_2$O** are disordered over two positions, and in this case, occupancies were refined to values 0.38:0.62 and 0.58:0.42, respectively. Structures were visualized by MERCURY [40], and the geometrical parameters were calculated by PLATON [41]. The crystallographic data for **1a·2H$_2$O**, **1b·2.5H$_2$O**, **2·4H$_2$O**, **3·8H$_2$O**, and **3·9H$_2$O** are summarized in Tables S1 and S2.

Powder X-ray Diffraction (PXRD). The Panalytical Aeris diffractometer was used to collect powder X-ray diffraction data in a Bragg–Brentano geometry. The source of radiation was CuKα (λ = 1.54056 Å). The sample was placed on a Si sample holder and measured. The experiment was conducted at 2θ = 5–40° with 0.022° and 15.045 s per step. Data were visualized by the DataViewer program [42].

***In vitro* cytotoxic activity.** Cytotoxicity experiments on compounds **1a·2H$_2$O** and **2·4H$_2$O** were performed at the School of Medicine, the University of Zagreb. Experiments were evaluated on two human cell lines: human hepatocellular carcinoma cell lines (HepG2) and human acute monocytic leukemia cancer cell lines (THP-1). The antiproliferative effects of compounds **1a·2H$_2$O** and **2·4H$_2$O** were determined by the CellTiter 96 Aqueous One Solution Cell Proliferation Assay (Promega, G3580). This is a tetrazolium-based cell viability assay that measures the metabolic capacity of cells in a culture [43]. **1a·2H$_2$O** and **2·4H$_2$O**

were prepared in sterilized water as a stock solution at a concentration of 10^{-2} mol dm^{-3}. Before their application into the bioassay, compounds were diluted in a cell culture medium. Cells were added to plates in an appropriate number per well (50 µL). Plates were incubated overnight at 37 °C in a 5% CO_2 atmosphere. For determining the inhibition of cellular proliferation or the inducement of cytotoxic effects, the CellTiter 96 Aqueous One Solution Cell Proliferation Assay (Promega, G3580) was used. A total of 10 µL of an MTS reagent was dispensed per well. Plates were incubated for 2 h at 37 °C in a 5% CO_2 atmosphere, and the absorbances were recorded at 490 nm using a 96-well Spectramax i3x plate reader. Results were analyzed in the GraphPad Prism software.

3. Results

3.1. Synthetic Comments

Five new ternary coordination compounds containing copper(II) ions; aminoacidate (L-alaninate (L-Ala), L-valinate (L-Val), or L-phenylalaninate (L-Phen)); and 2,2′-bipyridine (bipy) were prepared using a solution-based and/or mechanochemical synthesis, as listed in Figure 1. Two compounds with L-alaninate were synthesized under different conditions—**1b·2.5H$_2$O** was crystallized from an aqueous solution, while **1a·2H$_2$O** was crystallized from a methanolic solution. In some repeated experiments, **1b·2.5H$_2$O** was also crystallized from methanolic solution. By using a mechanochemical synthesis, only **1b·2.5H$_2$O** was prepared. In syntheses with L-valinate, only one compound was formed, **2·4H$_2$O**, both in aqueous and methanolic solutions, and mechanochemically with a small amount of water or methanol. L-Phenylalaninate produced compounds with a higher fraction of water, **3·8H$_2$O** and **3·9H$_2$O**, where the crystallization product depended on a solvent. No crystalline product was formed at a higher water ratio in the solution-based synthesis, while a mixture of water and methanol (1:9 *v*/*v*) gave crystals of **3·8H$_2$O**. From pure methanol, **3·9H$_2$O** was crystallized from a solution. In some experiments, [Cu(L-Phe)$_2$]$_n$ was crystallized from a solution, both from a mixture of water and methanol (1:9 *v*/*v*) or pure methanol, with the same number of reactants. **3·8H$_2$O** was synthesized mechanochemically when water was used for liquid-assisted grinding. A scheme of the synthetic procedures is given in Figure 1. The outcomes of solution-based syntheses involving alaninato and phenylalaninato ligands highly depended on unidentified external factors. In these cases, mechanochemical syntheses proved to be very useful in ensuring the reproducibility and purity of the bulk products.

3.2. Crystal Structures

The synthesized ternary coordination compounds are composed of complex cations of two different types, with sulfate counterions in **1a·2H$_2$O, 1b·2.5H$_2$O**, and **2·4H$_2$O** or of complex cations and complex anions in **3·8H$_2$O** and **3·9H$_2$O**, all of them being hydrates (Figures S4–S8). The asymmetric unit of **1a·2H$_2$O** consists of two octahedrally coordinated complex cations (with bridging alaninato ligands), two sulfate anions with an occupancy of 0.5, and two crystallization water molecules (Figure S4). In **1b·2.5H$_2$O,** the asymmetric unit contains two complex cations, one octahedrally coordinated (with bridging alaninato ligand) and another square-pyramidal, with two symmetrically unique halves of sulfate anions and 2.5 crystallization water molecules (Figure S5). In **1b·2.5H$_2$O**, sulfate anions and one water molecule lie on a 2-fold axis of rotation. The asymmetric unit of **2·4H$_2$O** contains one octahedrally coordinated (with bridging valinato ligand) and three square-pyramidal complex cations, two sulfate anions, and four crystallization water molecules (Figure S6). The **3·8H$_2$O** asymmetric unit contains four complex cations, four complex anions, and 32 crystallization water molecules (Figure S7), and **3·9H$_2$O** contains two complex cations, two complex anions, and 18 crystallization water molecules (Figure S8). In complex cations, the copper(II) ion is either pentacoordinated by one *N*,*O*-donating L-aminoacidato ligand and one *N*,*N*′-donating bipyridine ligand in the basal plane and an apically coordinated water molecule (in **1b·2.5H$_2$O**, **2·4H$_2$O**, **3·8H$_2$O**, and **3·9H$_2$O**; Figure 2a) or a hexacoordinated one, with the sixth position being occupied by a carboxylate

oxygen atom from a neighboring complex cation (in **1a·2H$_2$O**, **1b·2.5H$_2$O**, and **2·4H$_2$O**; Figure 2b). In complex anions, the copper atom is pentacoordinated by phenylalaninato and bipyridine ligands in the basal plane and apically coordinated in sulfate anions (in **3·8H$_2$O** and **3·9H$_2$O**; Figure 2c).

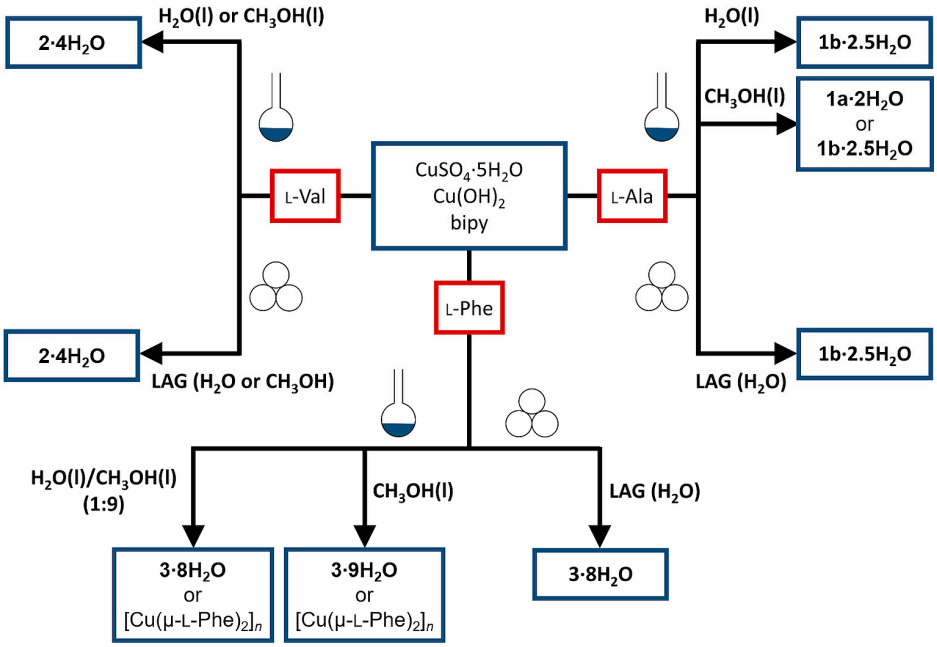

{[Cu(μ-L-Ala)(H$_2$O)(bipy)]$_2$SO$_4$·2H$_2$O}$_n$ (**1a·2H$_2$O**)
{[Cu(μ-L-Ala)(H$_2$O)(bipy)][Cu(L-Ala)(H$_2$O)(bipy)]SO$_4$·2.5H$_2$O}$_n$ (**1b·2.5H$_2$O**)
{[Cu(μ-L-Val)(H$_2$O)(bipy)][Cu(L-Val)(H$_2$O)(bipy)]$_3$(SO$_4$)$_2$·4H$_2$O}$_n$ (**2·4H$_2$O**)
[Cu(L-Phe)(H$_2$O)(bipy)][Cu(L-Phe)(SO$_4$)(bipy)]·8H$_2$O (**3·8H$_2$O**)
[Cu(L-Phe)(H$_2$O)(bipy)][Cu(L-Phe)(SO$_4$)(bipy)]·9H$_2$O (**3·9H$_2$O**)

Figure 1. Scheme of synthetic procedures for **1a·2H$_2$O**, **1b·2.5H$_2$O**, **2·4H$_2$O**, **3·8H$_2$O**, and **3·9H$_2$O**.

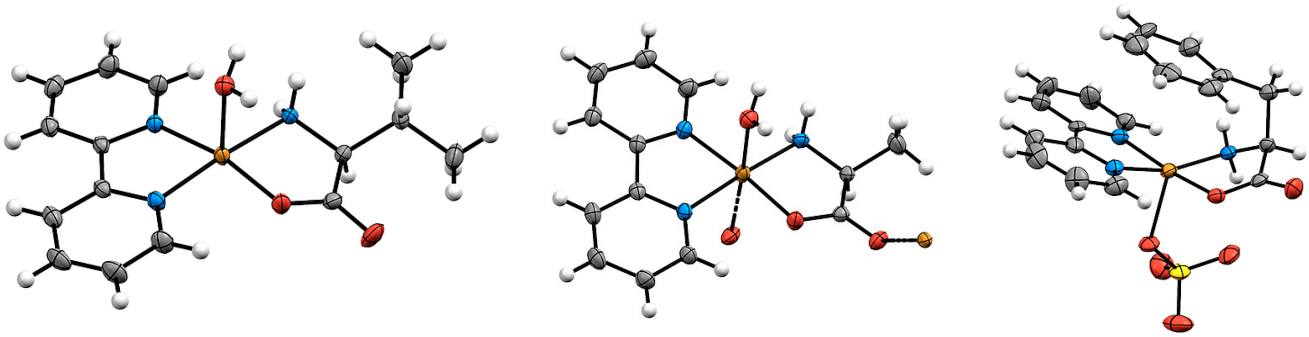

(**a**) (**b**) (**c**)

Figure 2. Different complex species in investigated coordination compounds: (**a**) complex cation in **2·4H$_2$O**; (**b**) polymeric complex cation in **1a·2H$_2$O**; (**c**) complex anion in **3·8H$_2$O**. Displacement ellipsoids are calculated at the 50% probability level.

In the equatorial plane, copper–oxygen bonds (1.927(2)—1.983(6) Å) are slightly shorter than copper–nitrogen bonds (1.966(5)–2.032(9) Å), which is consistent with literature data [44]. As expected for the copper(II) complexes, the pronounced Jahn–Teller effect is observed in all complex species, with elongated bonds in apical/axial positions. Additionally, both penta- and hexacoordinated complex species in L-alaninato and L-valinato coordination compounds, **1a·2H$_2$O**, **1b·2.5H$_2$O**, and **2·4H$_2$O**, have even longer

axial bonds (2.333(3)–2.874(4) Å) due to *trans*-influence. In all square–pyramidal complex species in these three compounds, either water or carboxylate oxygen atoms are in proximity of a copper atom (at a distance of 2.923(3)–3.324(4) Å) in *trans*-position to the apical ligand. L-Phenylalaninato coordination compounds, **3·8H$_2$O** and **3·9H$_2$O**, do not show *trans*-influence (distances of d(Cu–O$_{axial}$) = 2.181(7)–2.320(6) Å) due to the steric hindrance caused by the phenyl ring. Bond lengths in the coordination sphere of copper in all investigated compounds are given in Table 1. All of the pentacoordinated complex species are in elongated square–pyramidal geometry, with a different level of distortion (τ_5 parameters are 0.05–0.41). The τ_5 parameters are given in Table S3.

Table 1. Intramolecular bond lengths of copper(II) coordination sphere in compounds **1a·2H$_2$O**, **1b·2.5H$_2$O**, **2·4H$_2$O**, **3·8H$_2$O**, and **3·9H$_2$O**.

Compound	d(Cu–O$_{carboxylate}$)/Å	d(Cu–N$_{aminoacidate}$)/Å	d(Cu–N$_{bipyridine}$)/Å	d(Cu–O$_{water/sulfate}$)/Å	d(Cu–O$_{carboxylate}$)/Å
1a·2H$_2$O	1.950(2)	1.9863(18)	1.9984(18); 2.012(2)	2.430(2)	2.672(2) [2]
	1.961(2)	1.9816(18)	1.9982(18); 2.008(2)	2.419(2)	2.690(2) [3]
1b·2.5H$_2$O	1.933(5)	1.986(5)	1.994(5); 2.013(5)	2.457(6)	2.846(6) [4]
	1.955(5)	1.966(5)	1.994(5); 2.006(5)	2.394(6)	2.930(6) [1]
2·4H$_2$O	1.936(2)	1.992(3)	2.003(3); 2.004(3)	2.333(3)	3.324(4) [1]
	1.927(2)	1.988(2)	1.999(2); 2.004(3)	2.462(3)	3.134(4) [1]
	1.943(2)	1.982(2)	1.988(2); 2.005(3)	2.476(3)	2.923(3) [1]
	1.940(2)	1.985(3)	1.995(2); 1.990(3)	2.874(4)	2.573(3) [5]
3·8H$_2$O	1.970(7)	2.000(9)	2.002(9); 1.983(8)	2.224(7)	/
	1.983(6)	1.985(9)	2.005(9); 1.983(8)	2.274(7)	/
	1.966(7)	2.010(9)	1.994(9); 2.016(8)	2.215(9)	/
	1.964(7)	1.996(7)	1.995(7); 1.989(9)	2.194(7)	/
	1.956(7)	1.997(9)	1.995(9); 1.997(8)	2.281(7)	/
	1.959(9)	1.994(9)	2.004(10); 2.010(9)	2.219(7)	/
	1.945(8)	2.040(9)	2.006(9); 1.994(8)	2.236(9)	/
	1.962(8)	2.032(9)	2.009(9); 1.989(10)	2.186(7)	/
3·9H$_2$O	1.953(7)	1.992(7)	2.016(8); 2.006(7)	2.320(6)	/
	1.956(6)	2.015(7)	2.009(7); 1.988(8)	2.185(6)	/
	1.966(7)	1.990(9)	1.979(8); 2.003(8)	2.277(10)	/
	1.941(8)	2.023(9)	1.991(9); 2.007(9)	2.181(7)	/

[1] Cu···O distance bigger than the sum of van der Waals radii; [2] $1/2-x,1/2+y,-z$; [3] $1/2-x,-1/2+y,1-z$; [4] $-1/2+x,3/2-y,1-z$; [5] $1/2-x,1/2+y,2-z$.

In **3·8H$_2$O** and **3·9H$_2$O**, two types of conformations of L-phenylalaninato residue are observed: *gauche*$^-$ and *gauche*$^+$. Six symmetrically independent complex species in **3·8H$_2$O** (three complex cations and three complex anions) and three complex species in **3·9H$_2$O** (one complex cation and two complex anions) are in *gauche*$^-$ conformation (χ_1 angles, ∠(Nx–CxA–CxB–CxG1) and are in the range of 36.4(12)–65.9(10)°). The phenyl ring from the L-phenylalaninato residue is almost coplanar with the bipyridine ligand in the same complex (dihedral angles between planes of the phenyl ring and any of the bipyridine rings are 2.0(5)–14.4(5)°). Two symmetrically independent complex species in **3·8H$_2$O** (one complex cation and one complex anion) and one complex cation in **3·9H$_2$O** are in *gauche*$^+$ conformation (χ_1 angles, ∠(Nx–CxA–CxB–CxG1) and are in the range of −64.5(11) to −69.6(12)°). The torsion angles χ_1 (∠(Nx–CxA–CxB–CxG1)) are given in Table S4.

The crystal structures of the complex species can be divided into the hydrophobic part, with aliphatic side chains of alanine and valine and aromatic systems of bipyridine and phenylalanine ligands, and the hydrophilic part of aminoacidates, with water molecules and sulfate ions. Due to the specific structure, complex species form predictable supramolecular architectures. Complex cations in **1·2H$_2$O, 1·2.5H$_2$O**, and **2·4H$_2$O** are stacked into infinite 1D chains through π interactions between bipyridine ligands in the [010], [100],

and [010] directions, respectively. Within the chains, longer (4.6943(17)–5.7026(19) Å) and shorter (3.6398(19)–3.8319(16) Å) centroid···centroid distances are alternating between two bipyridine ligands (Tables S5 and S6). These chains are connected through coordination (d(Cu···$O_{carboxylate}$) = 2.573(3)–2.846(6) Å), carboxylate···copper intermolecular interactions (d(Cu···$O_{carboxylate}$) = 2.923(3)–3.324(4) Å), and O–H···$O_{carboxylate}$ hydrogen bonds (d(O–H···$O_{carboxylate}$) = 2.812(3)–2.985(4) Å) forming 2D supramolecular layers parallel to (10$\bar{1}$) in **1·2H$_2$O**, (010) in **1·2.5H$_2$O**, and (101) in **2·4H$_2$O** (Figure 3 and Tables 1 and S5–S7). Sulfate ions and crystallization water molecules act as hydrogen-bonding bridges between 2D layers.

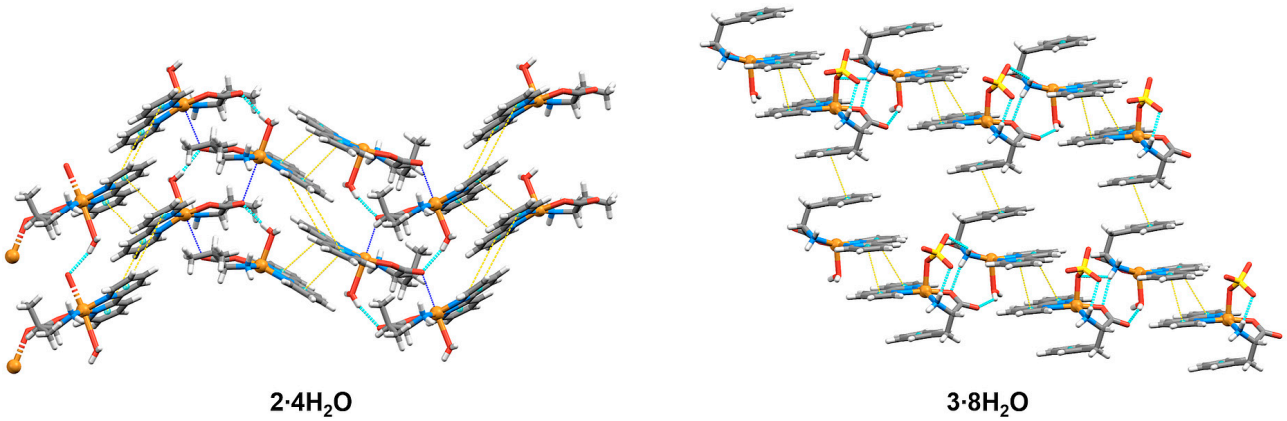

Figure 3. Two-dimensional layers in **2·4H$_2$O** and **3·8H$_2$O** formed by π interactions (yellow), carboxylate···copper interactions (blue; in **2·4H$_2$O**), and hydrogen bonds (cyan).

In **3·8H$_2$O** and **3·9H$_2$O**, complex cations and anions, which are in *gauche*$^-$ conformation, form 1D chains through π interactions (Tables S8 and S9) in the alternating fashion of the two bipyridine ligands (d(Cg···Cg) = 3.565(5)–4.012(6) Å) and the two phenyl rings (d(Cg···Cg) = 3.760(7)–4.060(6) Å). One-dimensional chains are connected through O–H···$O_{carboxylate}$ (d(O–H···$O_{carboxylate}$) = 2.633(11)–2.708(9) Å), N–H···$O_{carboxylate}$ (d(N–H···$O_{carboxylate}$) = 2.944(10)–3.151(12) Å), and N–H···$O_{sulfate}$ (d(N–H···$O_{sulfate}$) = 2.988(14)–3.138(11) Å) hydrogen bonds forming 2D supramolecular layers parallel to (010) (Figure 3, Table S7). Complex cations and anions in *gauche*$^+$ conformation form dimers (d(Cg···Cg) = 3.608(6)–4.843(6) Å) with one complex species in *gauche*$^-$ conformation. π-stacked dimers are connected through O–H···$O_{sulfate}$ (d(O–H···$O_{sulfate}$) = 2.671(11)–2.744(12) Å) and N–H···$O_{sulfate}$ (d(N–H···$O_{sulfate}$) = 2.916(14)–3.333(14) Å) hydrogen bonds forming 1D chains propagating along [001] in **3·8H$_2$O** and [100] in **3·9H$_2$O** (Figure 4, Table S7).

In all the compounds, crystallization water molecules are packed between 2D layers formed by coordination compounds. There is a significant difference in the amount and packing pattern of crystallization water molecules between compounds with aliphatic amino acids and phenylalanine compounds. **1a·2H$_2$O, 1b·2.5H$_2$O**, and **2·4H$_2$O** contain a lower fraction of water molecules (2.0, 5.3, and 4.4% of the unit cell volume, respectively), and the water molecules pack in discrete pockets (Figure 5). On the other hand, **3·8H$_2$O** and **3·9H$_2$O** contain higher amounts of water (20.9% and 22.4% of the unit cell volume, respectively), and the water molecules pack into 2D channels (Figure 5).

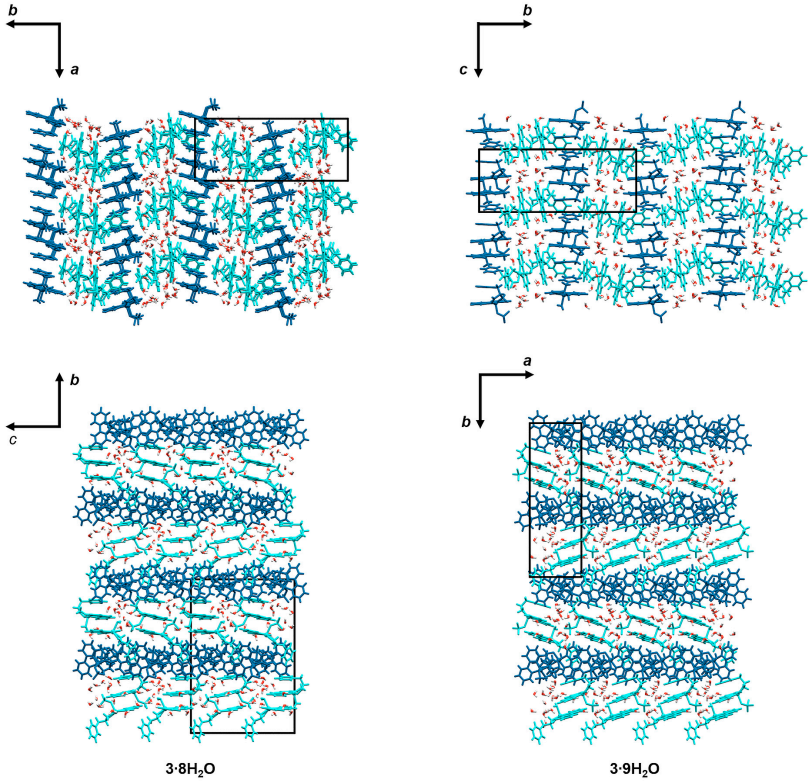

Figure 4. Crystal packing of **3·8H$_2$O** and **3·9H$_2$O**. Complex species form 2D layers (dark blue) parallel to the (010) plane in **3·8H$_2$O** and **3·9H$_2$O** and dimers connected by hydrogen bonds (light blue), which propagate along [001] in **3·8H$_2$O** and [100] in **3·9H$_2$O**.

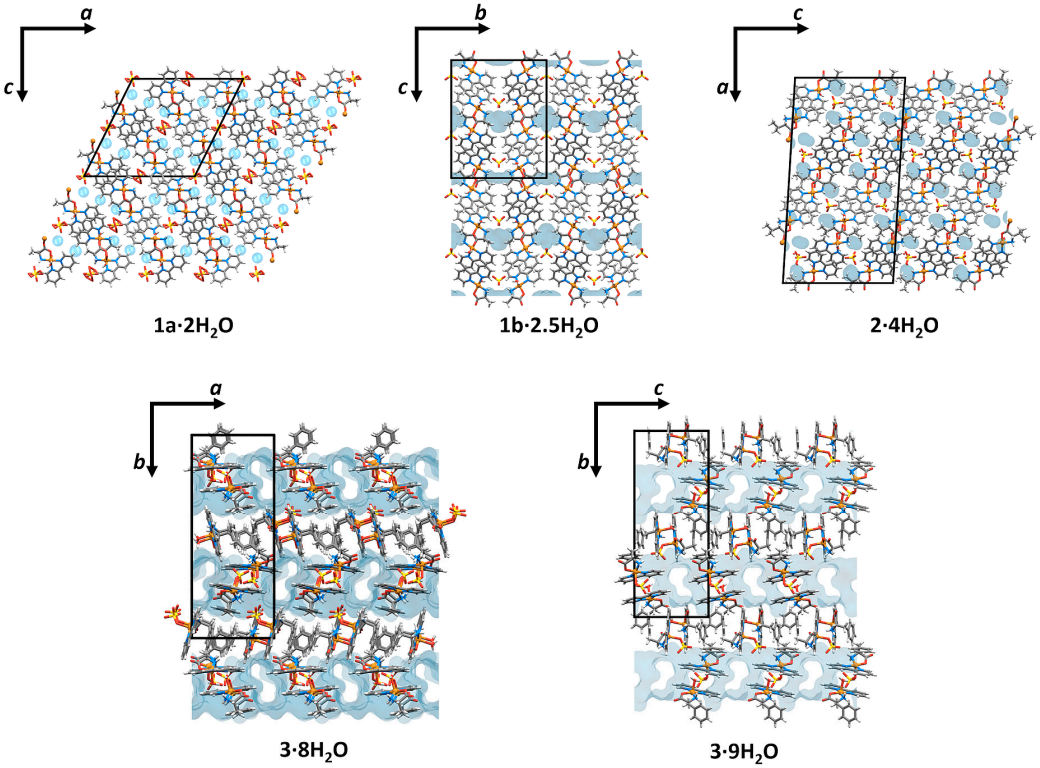

Figure 5. Crystal packing of **1a·2H$_2$O**, **1b·2.5H$_2$O**, **2·4H$_2$O**, **3·8H$_2$O**, and **3·9H$_2$O**. Surface around crystallization water molecules is shown in blue. Water molecules were omitted for clarity.

3.3. IR (ATR) Analysis

As explained in Section 3.1, we were not able to repeat the synthesis of compounds **1a·2H$_2$O** and **3·9H$_2$O** to obtain a pure bulk sample for the IR and TG analysis. Infrared and thermogravimetric analyses were made for **1b·2.5H$_2$O**, **2·4H$_2$O**, and **3·8H$_2$O**, for which we could reproduce pure samples (Figures S9–S11). As being built by analogous moieties that are almost identically coordinated to the copper(II) centers, the IR spectra of analyzed compounds are similar. Each compound shows one or two broad bands from 3450 cm^{-1} to 3150 cm^{-1} that may be assigned to ν(O–H) and ν(N–H) stretching vibrations. These bands indicate extensive hydrogen bonding in crystal structures. In a broad band in the range of 1690–1530 cm^{-1}, there is an overlap of several vibrational modes of the carboxylate group, the C=N, NH$_2$, and OH groups. Absorption bands from 1630 cm^{-1} to 1600 cm^{-1}, together with those from 1480 cm^{-1} to 1390 cm^{-1}, may be assigned to stretching vibrations of the carboxylate groups $\widetilde{\nu}_{asym}(COO^-)$ and $\widetilde{\nu}_{sym}(COO^-)$, respectively [21,23,45,46]. Absorption bands from 1590 cm^{-1} to 1490 cm^{-1} are assigned to ring stretching, C=N stretching (1568 cm^{-1}), and ring bending vibrations. Absorption bands at 1218–1203 cm^{-1} and broad bands between 1150 and 1000 cm^{-1} correspond to the S=O stretching modes of sulfate ions, and those from 1000 cm^{-1} to 600 cm^{-1} belong to ring–H out-of-plane bending, ring in-plane bending, and ring torsion modes. Bands at 557 cm^{-1} and 548 cm^{-1} correspond to stretching vibrations that indicate Cu–O bonding, while those close to 460 cm^{-1} indicate Cu–N bonding.

3.4. Thermogravimetric Analysis

The TGA for **1b·2.5H$_2$O**, **2·4H$_2$O**, and **3·8H$_2$O** was performed in the flow of pure oxygen in the temperature range of 25–800 °C at a rate of 10 K min^{-1} (Figures S12–S14). Although crystals of all compounds are basically stable in the air at room temperature, water loss in all samples starts approximately at 40 °C, especially in the case of **3·8H$_2$O**, due to its high water content. All samples exhibit complex degradation, and a loss of water is overlapped by a further decomposition of the compound. Only in the case of **1b·2.5H$_2$O** is loss of water completed at approximately 180 °C, giving a step of 11.0%, which is in good agreement with the theoretical value (10.2%).

For all samples, further degradation of the compound continues up to 400 °C and then abruptly ends (430 °C to 460 °C for **1b·2.5H$_2$O**; 400 °C to 430 °C for **2·4H$_2$O**; and 420 °C to 450 °C for **3·8H$_2$O**), leaving residues that slowly decompose up to 750 °C. The residues in crucibles are identified as CuO. Data on CuO contents and corresponding Cu contents are given in Table S10. In general, experimentally determined Cu contents are in good agreement with theoretical values.

3.5. Cytotoxic Activity

The results of the cell viability assay with IC_{50} values of the tested compounds **1a·2H$_2$O** and **2·4H$_2$O** showed substantial antiproliferative activity towards human hepatocellular carcinoma cell lines (HepG2) and some activity towards human acute monocytic leukemia cancer cell lines (THP-1) (Table 2). The activity of the two compounds towards both cell lines was almost identical, pointing to a negligible structural influence on their antitumor activity. In our previous work on the ternary coordination compounds of copper(II) with glycine (Gly) and 2,2′-bipyridine (bipy), the compounds [Cu(Gly)(H$_2$O)(bipy)][Cu(Gly)(SO$_4$)(bipy)]·6H$_2$O and [Cu(Gly)(H$_2$O)(bipy)]$_2$SO$_4$ showed pronounced antiproliferative activity toward a panel of six human cell lines (the HepG2, KATO III, Caco-2, MDA-MB-231, PANC-1, and MRC-5 cells). The most impaired was the HepG2 cell line at a 10^{-5} mol dm^{-3} concentration (74.5% reduction in cell growth) [31]. It was shown that copper(II) complexes with a diethylamino substituent and 2,2′-bipyridine exhibited high in vitro cytotoxicity towards breast cancer cell lines (MDA-MB-231) [47,48]. Similarly, copper(II) complexes with benzimidazole-derived scaffolds and heterocyclic bases (1,10-phenanthroline and 2,2′-bipyridine) showed in vitro cytotoxic activities on human breast cancer MCF-7 cell lines and a binding affinity for the HSA protein [49].

Table 2. In vitro cytotoxicity (IC_{50} values [1]) of compounds **1a·2H$_2$O** and **2·4H$_2$O**.

	IC_{50}/μmol L^{-1}	
	HepG2	**THP-1**
1a·2H$_2$O	79.4	21.86
2·4H$_2$O	68.87	25.78
staurosporine	36.38	0.39

[1] Concentration that causes 50% inhibition of cell growth.

4. Conclusions

We have shown that by using different solvents (methanol or water), different hydrates of ternary coordination compounds with copper, 2,2′-bypiridine and amino acidates (L-alaninate, L-valinate and L-phenylalanine), can be obtained: {[Cu(μ-L-Ala)(H$_2$O)(bipy)]$_2$SO$_4$·2H$_2$O}$_n$ (**1a·2H$_2$O**), {[Cu(μ-L-Ala)(H$_2$O)(bipy)][Cu(L-Ala)(H$_2$O)(bipy)]SO$_4$·2.5H$_2$O}$_n$ (**1b·2.5H$_2$O**), {[Cu(μ-L-Val)(H$_2$O)(bipy)][Cu(L-Val)(H$_2$O)(bipy)]$_3$(SO$_4$)$_2$·4H$_2$O}$_n$ (**2·4H$_2$O**), [Cu(L-Phe)(H$_2$O)(bipy)][Cu(L-Phe)(SO$_4$)(bipy)]·8H$_2$O (**3·8H$_2$O**), and [Cu(L-Phe)(H$_2$O)(bipy)][Cu(L-Phe)(SO$_4$)(bipy)]·9H$_2$O (**3·9H$_2$O**). Solution-based syntheses of **1a·2H$_2$O**, **3·8H$_2$O**, and **3·9H$_2$O** were shown to be difficult to reproduce and to obtain pure products. On the other hand, mechanochemical syntheses proved to be a simple and reliable technique for obtaining **1b·2.5H$_2$O**, **2·4H$_2$O**, and **3·8H$_2$O**. Regarding the crystal structures, there is an influence of amino acid residue on crystal packing, with a clear difference in forming complex species and the packing of aliphatic (**1a·2H$_2$O**, **1b·2.5H$_2$O**, and **2·4H$_2$O**) and aromatic amino acids (**3·8H$_2$O** and **3·9H$_2$O**). Despite these differences, some similarities and predictability in the packing of aliphatic and phenylalaninato complexes are evident. The aromatic parts of complexes stack into rods, while carboxylate groups are bonded to a neighboring complex through hydrogen bonds in all of the prepared compounds. In similar synthetic conditions, L-phenylalaninate gave compounds with a significantly higher fraction of crystallization water molecules compared to the L-alaninato and L-valinato compounds. Like other *Casiopeina* compounds, **1a·2H$_2$O** and **2·4H$_2$O** exhibited significant antiproliferative activity towards human hepatocellular carcinoma cell lines (HepG2) and moderate activity towards human acute monocytic leukemia cancer cell lines (THP-1) compared to staurosporine. Both compounds have similar activity, with **1a·2H$_2$O** being slightly more active towards THP-1 and **2·4H$_2$O** towards the HepG2 cell line.

Supplementary Materials: The following supporting information can be downloaded at: https://www.mdpi.com/article/10.3390/cryst14070656/s1, Table S1: Crystallographic data for compounds **1a·2H$_2$O**, **1b·2.5H$_2$O**, and **2·4H$_2$O**; Table S2: Crystallographic data for compounds **3·8H$_2$O** and **3·9H$_2$O**; Table S3: Geometries and τ_5 parameters of complex cations and anions in **1a·2H$_2$O**, **1b·2.5H$_2$O**, **2·4H$_2$O**, **3·8H$_2$O**, and **3·9H$_2$O**; Table S4: Torsion angles and conformation of phenylalaninate in **3·8H$_2$O** and **3·9H$_2$O**; Table S5: Geometric parameters of the aromatic rings stacked by π interactions in **1a·2H$_2$O** and **1b·2.5H$_2$O**; Table S6: Geometric parameters of the aromatic rings stacked by π interactions in **2·4H$_2$O**: Table S7: Inter- and intramolecular hydrogen bonds within π-stacked 2D layers in **1a·2H$_2$O**, **1b·2.5H$_2$O**, **2·4H$_2$O**, **3·8H$_2$O**, and **3·9H$_2$O**; Table S8: Geometric parameters of the aromatic rings stacked by π interactions in **3·8H$_2$O**; Table S9: Geometric parameters of the aromatic rings stacked by π interactions in **3·9H$_2$O**; Table S10: Overview of theoretical and experimentally determined water and copper contents in samples of **1b·2.5H$_2$O**, **2·4H$_2$O**, and **3·8H$_2$O**; Figure S1: Powder diffraction pattern of a sample obtained by the mechanochemical synthesis of **1b·2.5H$_2$O** (blue) compared to the powder diffraction pattern of **1b·2.5H$_2$O** simulated from the crystal structure data (red); Figure S2: Powder diffraction pattern of a sample obtained by the mechanochemical synthesis of **2·4H$_2$O** with methanol (purple) or water (blue) compared to the powder diffraction pattern of **2·4H$_2$O** simulated from the crystal structure data (red); Figure S3: The powder diffraction pattern of a sample obtained by the mechanochemical synthesis of **3·8H$_2$O** and aging in the air for 5 min (dark blue), 10 min (blue), and 3 months (light blue) prior to measurements compared to the powder diffraction patterns of **3·8H$_2$O** (red) and **3·9H$_2$O** (black) simulated from the crystal structure data; Figure S4: ORTEP plot of the asymmetric unit of **1a·2H$_2$O** with the atom-labelling scheme. Crystallization water molecules were omitted for clarity. Sulfate atoms are disordered in two

positions. Displacement ellipsoids were calculated at the 50% probability level. Symmetry operators: $^{i}1/2-x,-1/2+y,-z$; $^{ii}1/2-x,1/2+y,-z$; $^{iii}1/2-x,1/2+y,1-z$; $^{iv}1/2-x,-1/2+y,1-z$; ^{v} $x,y,1-z$; $^{vi}-x,y,-z$; Figure S5: ORTEP plot of the asymmetric unit of **1b·2.5H$_2$O** with the atom-labelling scheme. Crystallization water molecules were omitted for clarity. Displacement ellipsoids were calculated at the 50% probability level. Symmetry operators: $^{i}-1/2+x,3/2-y,1-z$; $^{ii}1/2+x,3/2-y,1-z$; Figure S6: (a) ORTEP plot of the asymmetric unit of **2·4H$_2$O** and (b) the atom-labelling scheme of two complex species. Crystallization water molecules and two other complex cations in (b) were omitted for clarity. One sulfate ion and one side chain of L-valinate is disordered in two positions. Displacement ellipsoids were calculated at the 50% probability level. Symmetry operators: $^{i}1/2-x,1/2+y,2-z$; $^{ii}1/2-x,-1/2+y,2-z$; Figure S7: (a) ORTEP plot of the asymmetric unit of **3·8H$_2$O** and (b) the atom-labelling scheme of two complex species. Crystallization water molecules and six complex species in (b) were omitted for clarity. Displacement ellipsoids were calculated at the 50% probability level; Figure S8: (a) ORTEP plot of the asymmetric unit of **3·9H$_2$O**, and (b) the atom-labelling scheme of two complex species. Crystallization water molecules and two complex species in (b) were omitted for clarity. Displacement ellipsoids were calculated at the 50% probability level; Figure S9: IR(ATR) spectrum of **1b·2.5H$_2$O**; Figure S10: IR(ATR) spectrum of **2·4H$_2$O**; Figure S11: IR(ATR) spectrum of **3·8H$_2$O**; Figure S12: TGA curve of **1b·2.5H$_2$O**; Figure S13: TGA curve of **2·4H$_2$O**; Figure S14: TGA curve of **3·8H$_2$O**. CCDCs 2363904–2363908 contain the supplementary crystallographic data for this paper. These data can be obtained free of charge via http://www.ccdc.cam.ac.uk/structures (accessed on 14 July 2024) or from the CCDC, 12 Union Road, Cambridge CB2 1EZ, UK; Fax: +44 1223 336033; E-mail: deposit@ccdc.cam.ac.uk.

Author Contributions: Conceptualization, D.V. and B.P.; methodology, D.V., N.J., K.L. and B.P.; validation, D.V., N.J. and B.P.; formal analysis, D.V., K.L., N.J. and B.P.; investigation, D.V., K.L., N.J. and B.P.; resources, D.V., N.J. and B.P.; data curation, D.V., K.L., N.J. and B.P.; writing—original draft preparation, D.V., K.L., N.J. and B.P.; visualization, D.V. and B.P.; supervision, B.P.; project administration, B.P.; funding acquisition, B.P. All authors have read and agreed to the published version of the manuscript.

Funding: This research was funded by project CIuK, which was co-financed by the Croatian Government and the European Union through the European Regional Development Fund–Competitiveness and Cohesion Operational Programme (Grant KK.01.1.1.02.0016) and by an institutional project financed by the University of Zagreb entitled Synthesis and Structural Characterization of Organic and Complex Compounds: Protein Structure.

Data Availability Statement: The original contributions presented in the study are included in the article and Supplementary Materials, further inquiries can be directed to the corresponding author.

Conflicts of Interest: The authors declare no conflicts of interest.

References

1. Ruiz-Azuara, L.; Bravo-Gomez, M.E. Copper Compounds in Cancer Chemotherapy. *Curr. Med. Chem.* **2010**, *17*, 3606–3615. [CrossRef] [PubMed]
2. Milanino, R.; Buchner, V. Copper: Role of the 'Endogenous' and 'Exogenous' Metal on the Development and Control of Inflammatory Processes. *Rev. Environ. Health* **2006**, *21*, 153–215. [CrossRef] [PubMed]
3. Rodrigues, T.A.D.; de Arruda, E.J.; Fernandes, M.F.; de Carvalho, C.T.; Lima, A.R.; Cabrini, I. Copper II—Polar amino acid complexes: Toxicity to bacteria and larvae of *Aedes aegypti*. *An. Acad. Bras. Cienc.* **2017**, *89*, 2273–2280. [CrossRef] [PubMed]
4. Iakovidis, I.; Delimaris, I.; Piperakis, S.M. Copper and Its Complexes in Medicine: A Biochemical Approach. *Mol. Biol. Int.* **2011**, *2011*, 594529. [CrossRef] [PubMed]
5. Bikas, R.; Soltani, B.; Sheykhi, H.; Korabik, M.; Hossaini-Sadr, M. Synthesis, crystal structure and magneto-structural studies of 2D copper(II) coordination polymer containing L-alanine amino acid. *J. Mol. Struct.* **2018**, *1168*, 195–201. [CrossRef]
6. Vušak, D.; Prugovečki, B.; Milić, D.; Marković, M.; Petković, I.; Kralj, M.; Matković-Čalogović, D. Synthesis and Crystal Structure of Solvated Complexes of Copper(II) with Serine and Phenanthroline and Their Solid-State-to-Solid-State Transformation into One Stable Solvate. *Cryst. Growth Des.* **2017**, *17*, 6049–6061. [CrossRef]
7. Smokrović, K.; Muratović, S.; Karadeniz, B.; Užarević, K.; Žilić, D.; Đilović, I. Synthon Robustness and Structural Modularity of Copper(II) Two-Dimensional Coordination Polymers with Isomeric Amino Acids and 4,4′-Bipyridine. *Cryst. Growth Des.* **2020**, *20*, 2415–2423. [CrossRef]
8. Chikira, M.; Ng, C.; Palaniandavar, M. Interaction of DNA with Simple and Mixed Ligand Copper(II) Complexes of 1,10-Phenanthrolines as Studied by DNA-Fiber EPR Spectroscopy. *Int. J. Mol. Sci.* **2015**, *16*, 22754–22780. [CrossRef] [PubMed]

9. Titova, Y. Transition Metal Complexes with Amino Acids, Peptides and Carbohydrates in Catalytic Asymmetric Synthesis: A Short Review. *Processes* **2024**, *12*, 214. [CrossRef]
10. Ma, D.; Cai, Q. Copper/Amino Acid Catalyzed Cross-Couplings of Aryl and Vinyl Halides with Nucleophiles. *Acc. Chem. Res.* **2008**, *41*, 1450–1460. [CrossRef]
11. Rosenberg, B.; VanCamp, L. The successful regression of large solid sarcoma 180 tumors by platinum compounds. *Cancer Res.* **1970**, *30*, 1799–1802. [PubMed]
12. Marín-Hernández, A.; Gallardo-Pérez, J.C.; López-Ramírez, S.Y.; García-García, J.D.; Rodríguez-Zavala, J.S.; Ruiz-Ramírez, L.; Gracia-Mora, I.; Zentella-Dehesa, A.; Sosa-Garrocho, M.; Macías-Silva, M.; et al. Casiopeina II-gly and bromo-pyruvate inhibition of tumor hexokinase, glycolysis, and oxidative phosphorylation. *Arch. Toxicol.* **2012**, *86*, 753–766. [CrossRef] [PubMed]
13. Santini, C.; Pellei, M.; Gandin, V.; Porchia, M.; Tisato, F.; Marzano, C. Advances in Copper Complexes as Anticancer Agents. *Chem. Rev.* **2014**, *114*, 815–862. [CrossRef] [PubMed]
14. Haleel, A.; Mahendiran, D.; Veena, V.; Sakthivel, N.; Rahiman, A.K. Antioxidant, DNA interaction, VEGFR2 kinase, topoisomerase I and in vitro cytotoxic activities of heteroleptic copper(II) complexes of tetrazolo[1,5-a]pyrimidines and diimines. *Mater. Sci. Eng. C* **2016**, *68*, 366–382. [CrossRef] [PubMed]
15. Erxleben, A. Interactions of copper complexes with nucleic acids. *Coord. Chem. Rev.* **2018**, *360*, 92–121. [CrossRef]
16. Garcia, H.C.; Cunha, R.T.; Diniz, R.; de Oliveira, L.F.C. Co-crystal and crystal: Supramolecular arrangement obtained from 4-aminosalicylic acid, bpa ligand and cobalt ion. *J. Mol. Struct.* **2012**, *1010*, 104–110. [CrossRef]
17. Subramanian, P.S.; Suresh, E.; Dastidar, P.; Waghmode, S.; Srinivas, D. Conformational Isomerism and Weak Molecular and Magnetic Interactions in Ternary Copper(II) Complexes of [Cu(AA)L′]$ClO_4 \cdot nH_2O$, Where AA = L-Phenylalanine and L-Histidine, L′ = 1,10-Phenanthroline and 2,2-Bipyridine, and n = 1 or 1.5: Synthesis, Single-Crystal X-ray Structures, and Magnetic Resonance Investigations. *Inorg. Chem.* **2001**, *40*, 4291–4301. [CrossRef]
18. Solans, X.; Ruíz-Ramírez, L.; Martínez, A.; Gasque, L.; Moreno-Esparza, R. Mixed chelate complexes. III. Structures of (L-alaninato)(aqua)(2,2′-bipyridine)copper(II) nitrate monohydrate and aqua(2,2′-bipyridine)(L-tyrosinato)copper(II) chloride trihydrate. *Acta Crystallogr. Sect. C Cryst. Struct. Commun.* **1992**, *48*, 1785–1788. [CrossRef]
19. Braban, M.; Haiduc, I.; Lönnecke, P. catena-Poly[[[(2,2′-bipyridyl)copper(II)]-μ-L-alaninato] perchlorate monohydrate]. *Acta Crystallogr. Sect. E Struct. Rep. Online* **2009**, *65*, m51. [CrossRef]
20. Zhang, W.C.; Lu, X. Long-lived photoluminescence and high quantum yield of copper(II) complexes with novel nanostructures. *RSC Adv.* **2015**, *5*, 101155–101161. [CrossRef]
21. Hua Zhou, X.; Yi Le, X.; Chen, S. Synthesis, crystal structure and properties of a one-dimensional L-valinate bridged coordination polymer: $[Cu_2(\text{L-val})_2(bpy)_2]_n \cdot 2nClO_4 \cdot 2nH_2O$. *J. Coord. Chem.* **2005**, *58*, 993–1001. [CrossRef]
22. Subramanian, P.S.; Suresh, E.; Casella, L. Supramolecular Helical Architectures Dictated by Folded and Extended Conformations of the Amino Acid in Ternary Cu II/Diamine/Racemic Amino Acid Complexes. *Eur. J. Inorg. Chem.* **2007**, *2007*, 1654–1660. [CrossRef]
23. Shaban, S.Y.; Ramadan, A.E.-M.M.; Ibrahim, M.M.; Elshami, F.I.; van Eldik, R. Square planar versus square pyramidal copper(II) complexes containing N_3O moiety: Synthesis, structural characterization, kinetic and catalytic mimicking activity. *Inorganica Chim. Acta* **2019**, *486*, 608–616. [CrossRef]
24. Sugimori, T.; Masuda, H.; Ohata, N.; Koiwai, K.; Odani, A.; Yamauchi, O. Structural Dependence of Aromatic Ring Stacking and Related Weak Interactions in Ternary Amino Acid−Copper(II) Complexes and Its Biological Implication. *Inorg. Chem.* **1997**, *36*, 576–583. [CrossRef]
25. Haldar, R.; Kumar, A.; Mallick, B.; Ganguly, S.; Mandal, D.; Shanmugam, M. Discrete Molecular Copper(II) Complex for Efficient Piezoelectric Energy Harvesting Above Room-Temperature. *Angew. Chemie Int. Ed.* **2023**, *62*, e202216680. [CrossRef] [PubMed]
26. Haldar, R.; Kumar, A.; Mandal, D.; Shanmugam, M. Deciphering the anisotropic energy harvesting responses of an above room temperature molecular ferroelectric copper(II) complex single crystal. *Mater. Horiz.* **2024**, *11*, 454–459. [CrossRef] [PubMed]
27. Walkowiak, Z.; Gągor, A.; Soliman, S.M.; Jerzykiewicz, M.; Sarewicz, M.; Fitta, M.; Pełka, R.; Wojciechowska, A. New heteroleptic L-argininato copper(II) complex with bromide and *N*,*N*–heterocyclic ligands—Synthesis, supramolecular, spectroscopic, magnetic and theoretical investigations. *J. Mol. Struct.* **2024**, *1308*, 138094. [CrossRef]
28. Wojciechowska, A.; de Graaf, C.; Rojek, T.; Jerzykiewicz, M.; Malik, M.; Gągor, A.; Duczmal, M. A rare diiodo-L-tyrosine copper(II) complexes—Crystal and molecular structure of materials stabilized by weak interactions. *Polyhedron* **2022**, *219*, 115780. [CrossRef]
29. Ramírez-Contreras, D.; García-García, A.; Mendoza, A.; Serrano-de la Rosa, L.E.; Sánchez-Gaytán, B.L.; Melendez, F.J.; Castro, M.E.; González-Vergara, E. D,L-Citrullinato-bipyridine Copper Complex: Experimental and Theoretical Characterization. *Crystals* **2023**, *13*, 1391. [CrossRef]
30. Wojciechowska, A.; Rojek, T.; Misiaszek, T.; Gągor, A.; Rytlewski, P. The supramolecular hybrid inorganic–organic L-argininato-based copper(II) materials—Preparation, structural, spectroscopic and thermal properties. *Inorganica Chim. Acta* **2023**, *557*, 121698. [CrossRef]
31. Vušak, D.; Mišković Špoljarić, K.; Jurec, J.; Žilić, D.; Prugovečki, B. Ternary Coordination Compounds of Copper(II) with Glycine and 2,2′-bipyridine: Synthesis, Structural Characterization, Magnetic and Biological Properties. *Croat. Chem. Acta* **2023**, *95*, 157–165. [CrossRef]
32. Vušak, D.; Ležaić, K.; Jurec, J.; Žilić, D.; Prugovečki, B. Solvent effects on the crystallization and structure of ternary copper(II) coordination compounds with L-threonine and 1,10-phenanthroline. *Heliyon* **2022**, *8*, e09556. [CrossRef]

33. Agte, A.N.; Golynko, N.S. Production of chemically-pure $Cu(OH)_2$ and $Cu(OAc)_2$. Determination of the solubility of $Cu(OAc)_2$ in water. Production of technical $Cu(OAc)_2$. *Tr. Leningr. Khim. Tekh. Inst.* **1940**, *8*, 140–149.
34. Glemser, O.; Sauer, H. Copper(II) Hydroxide. In *Handbook of Preparative Inorganic Chemistry*, 2nd ed.; Brauer, G., Ed.; Academic Press Inc.: New York, NY, USA, 1965; Volume 2, pp. 1013–1014.
35. Van der Helm, D.; Lawson, M.B.; Enwall, E.L. The crystal structure of bis-(L-phenylalaninato)copper(II). *Acta Crystallogr. Sect. B Struct. Crystallogr. Cryst. Chem.* **1971**, *27*, 2411–2418. [CrossRef]
36. *CrysAlisPRO Software System*, version 1.171.43.105a; Rigaku Oxford Diffraction: Yarnton, UK, 2024.
37. Sheldrick, G.M. A short history of SHELX. *Acta Crystallogr. Sect. A Found. Crystallogr.* **2008**, *64*, 112–122. [CrossRef] [PubMed]
38. Sheldrick, G.M. Crystal structure refinement with SHELXL. *Acta Crystallogr. Sect. C Struct. Chem.* **2015**, *71*, 3–8. [CrossRef] [PubMed]
39. Farrugia, L.J. WinGX and ORTEP for Windows: An update. *J. Appl. Crystallogr.* **2012**, *45*, 849–854. [CrossRef]
40. Macrae, C.F.; Sovago, I.; Cottrell, S.J.; Galek, P.T.A.; McCabe, P.; Pidcock, E.; Platings, M.; Shields, G.P.; Stevens, J.S.; Towler, M.; et al. Mercury 4.0: From visualization to analysis, design and prediction. *J. Appl. Crystallogr.* **2020**, *53*, 226–235. [CrossRef]
41. Spek, A.L. Structure validation in chemical crystallography. *Acta Crystallogr. Sect. D Biol. Crystallogr.* **2009**, *65*, 148–155. [CrossRef]
42. *DataViewer*, version 1.9a; PANalytical B.V.: Almelo, The Nederlands, 2018.
43. Mosmann, T. Rapid colorimetric assay for cellular growth and survival: Application to proliferation and cytotoxicity assays. *J. Immunol. Methods* **1983**, *65*, 55–63. [CrossRef]
44. Groom, C.R.; Bruno, I.J.; Lightfoot, M.P.; Ward, S.C. The Cambridge Structural Database. *Acta Crystallogr. Sect. B Struct. Sci. Cryst. Eng. Mater.* **2016**, *72*, 171–179. [CrossRef] [PubMed]
45. Nakamoto, K. *Infrared and Raman Spectra of Inorganic and Coordination Compounds*; John Wiley & Sons, Inc.: Hoboken, NJ, USA, 2008; ISBN 9780470405840.
46. Gorduk, S.; Yilmaz, H.; Andac, O. Cu(II) and Cd(II) coordination polymers derived from pyrazine-2,3-dicarboxylato and 1-vinylimidazole ligands: Synthesis, characterization and hydrogen storage capacities. *Maced. J. Chem. Chem. Eng.* **2019**, *38*, 19. [CrossRef]
47. Rafi, U.M.; Mahendiran, D.; Devi, V.G.; Doble, M.; Rahiman, A.K. Pyridazine-based heteroleptic copper(II) complexes as potent anticancer drugs by inducing apoptosis and S-phase arrest in breast cancer cell. *Inorganica Chim. Acta* **2018**, *482*, 160–169. [CrossRef]
48. Ji, P.; Wang, P.; Chen, H.; Xu, Y.; Ge, J.; Tian, Z.; Yan, Z. Potential of Copper and Copper Compounds for Anticancer Applications. *Pharmaceuticals* **2023**, *16*, 234. [CrossRef]
49. Hussain, A.; AlAjmi, M.F.; Rehman, M.T.; Amir, S.; Husain, F.M.; Alsalme, A.; Siddiqui, M.A.; AlKhedhairy, A.A.; Khan, R.A. Copper(II) complexes as potential anticancer and Nonsteroidal anti-inflammatory agents: In vitro and in vivo studies. *Sci. Rep.* **2019**, *9*, 5237. [CrossRef]

Disclaimer/Publisher's Note: The statements, opinions and data contained in all publications are solely those of the individual author(s) and contributor(s) and not of MDPI and/or the editor(s). MDPI and/or the editor(s) disclaim responsibility for any injury to people or property resulting from any ideas, methods, instructions or products referred to in the content.